



The Synthesis of New Corrosion Inhibitors Based on Modified Chitosan to Provide Protection over Mild Steel



Elsayed Fouad ^a, Mohamed Abd El-Moneim ^b, Mahmoud El-Desouky ^c, and W.I. El-DougDoug ^{d,*}

^{a,c} Faculty of Engineering, Banha University, Egypt

^b Chemistry Department, Faculty of Science, Port Said University, Egypt

^d Chemistry Department, Faculty of Science, Benha University, Egypt

Abstract

Synthetization and evaluation of new chitosan derivatives to work as corrosion inhibitors for mild steel in acidic medium. The synthetization process was checked by Fourier-transformed infrared (FTIR) and the inhibition parameters were screened out by electrochemical measurements as well as surface change according to corrosion or forming a protective film was detected via scanning electron microscope (SEM) and X-ray dispersion. The inhibition efficiency increases with increasing the concentration of the inhibitor and with lowering temperature. The inhibition efficiency reached about 96.5% and showed enhancement comparable to chitosan only which reflected to the corrosion rate decreasing. The inhibition was interpreted due to the adsorption of chitosan derivatives on the surface of mild steel. The correlation between concentration of new chitosan derivatives and the inhibition effect was investigated by Potentiodynamic polarization. The adsorption nature of the inhibitor on the metal surface also checked according to Langmuir isotherm.

Keywords: Chitosan, Benzaldehyde, m-Nitro benzaldehyde, HCl, Steel, Potentiodynamic polarization

1. Introduction

In last decades, Mild steel became a pillar upon which many industries are based like structural steel, signs, automobiles, furniture, fencing, and much more. But the only defect facing that metal is its' ease of erosion in corrosive solutions [1-3].

This problem attracted many researchers to find a suitable, durable and cheap solution like coating by corrosion inhibitors or cathodic and anodic protection [4, 5]. But the ideal solution from the economical view and the availability to apply was the usage of inhibitors;

We can classify these corrosive inhibitors into categories according to several parameters like their chemical nature: synthetic organic and inorganic materials or natural extracts. The usage of corrosion inhibitors in a try to control metallic surfaces corrosion that are in a corrosive environment is a crucial point for many researchers [6-11]. A huge number of organic synthesized compounds have been evaluated to screen out their corrosion inhibition ability. Most of these studies concluded that the

synthetized organic compounds, particularly those have aromatic rings and functional heterocompounds like N, S and O, have shown higher inhibition efficiency[5, 11-13]. But many problems blocked the way in front of synthesis of these organic materials, like its safety to human health, so the synthesis of safe and inexpensive organic inhibitors is a necessity to provide a realistic solution to this problem.

Chitosan is one of these compounds that give inhibition effect[14] and it also considered as bio-polymers and natural extract as it could be extracted from the shells of seafood waste of crustaceans and also from the cell walls of some fungi like zygomycetes class as well as in the green algae like Chlorella species. Chemically, it is the result of N -deacetylation of polysaccharide called chitin and it is compound is formed of glucosamine and N -acetyl glucosamine repeated units linked by 1, 4 bond[15].

Chitosan derivatives are also used to prevent corrosion of pipeline steel in seawater and the

* Corresponding Author E-mail: eldougDoug1@gmail.com; (W.I. El-DougDoug).

EJCHEM use only: Received date 16 March 2022; revised date 29 April 2022; accepted date 08 May 2022

DOI: 10.21608/EJCHEM.2022.127782.5668

©2023 National Information and Documentation Center (NIDOC)

anticorrosive effect of chitosan is due to its amine and hydroxyl groups. However, studies showed that Chitosan has a modest efficiency of inhibition. So, the enhancement of this efficiency takes a lot of efforts by synthesis Chitosan derivatives [14, 16-21].

2. Methodology

2.1. Instrumentation

The earliest tests used polarization and potentiostatic devices to examine the measurement of anticorrosive characteristics. The inspection is carried out with the help of three electrode sections, working electrode platinum electrode and reference electrode fabricated from saturated calomel electrode. In the polarization experiments .The electrode was immersed in the test solution until the steady state potential is attained and then start the polarization .It was found that the suitable time is 30 minutes and hence the polarization is started.

The potential range was scanned at a rate of 10 mV^s⁻¹ from -0.6 to 0.6 Volts, and the mild steel sample was manufactured with an exposure area of 1 cm² and then submerged in various HCl samples. The potentiostatic polarization measurements were carried out using a PS remote potentiostat with PS6 software to compute the corrosion parameters at a scanning rate 2mVsec⁻¹. The measurements were conducted in a stagnant medium.

Table 1
Chemical Composition of mild steel

Element	C	Mn	P	Si	S	Cr	Ni	Fe
Weight %	0.158	0.495	0.060	0.157	0.062	0.047	0.006	rest

Different grades of sheets (1200–2000) were used to abrade the metal surfaces, which were subsequently degreased with AR-grade acetone, cleaned with deionized water, and added to the test solution. Parameters including corrosion potential (E_{corr}), Corrosion current density (I_{corr}) were identified by Tafel curves extrapolation. The inhibition efficiency is calculated from

$$IE \% = \frac{I_{free} - I_{inh}}{I_{free}} * 100$$

Where the I_{free} and I_{inh} are the corrosion current densities before and after exposure to different inhibitors.

Infrared spectroscopy was used to identify the functional groups in the new synthesized resins and compounds.

Thermo Fisher Scientific's FTIR Nicolet Magna 5PC spectrophotometer was used to detect the IR spectra and identify the functional groups in the newly produced resins and compounds.

2.2. Chemicals

Chitosan with average molecular weight of 160000 g. Mol⁻¹, benzaldehyde and m-nitrobenzaldehyde were purchased from Sigma Aldrich Co. Hydrochloric acid (30 – 34) % was purchased from El-NASR Co.

2.3. Synthesis

One gram of Chitosan was dissolved in 100 ml of acetic acid solution (1%) on cold for about half hour, then the addition of 20 ml drop by drop of derivative solution (1gm of derivative dissolved in 20 ml methanol) then stirring for about 2 hours on cold by using a magnetic stirrer.

Then reflux in water bath (60°C - 70°C) for 12 hours. After complete precipitation of derivative chitosan, addition steps of washing and filtration were done to increase the purity of the compound.

2.3.1. Synthesis of m-nitrobenzaldehyde modified Chitosan resin

By using a m-nitrobenzaldehyde solution in synthesis scheme, the precipitation resulted was dried to give a final product of a pale-yellow powder of m-nitrobenzaldehyde chitosan.

2.3.2. Synthesis of benzaldehyde modified Chitosan resin

By using a benzaldehyde solution in synthesis scheme, the precipitation resulted was dried to give a final product of a pale-yellow powder of benzaldehyde chitosan.

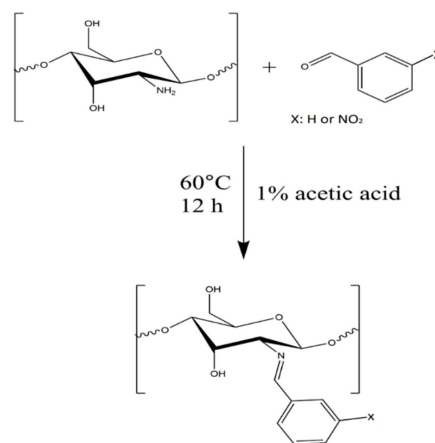


Figure 1: Synthesis of benzaldehyde chitosan and m-nitrobenzaldehyde chitosan

3. Results and Discussion

3.1. FTIR Spectrum explanation

The FTIR spectrum of chitosan shows broad band at [3428-3440] cm^{-1} related to the OH functional group, the cyclic C-O-C group appears at [810-950] cm^{-1} , the bands of [1070-1080] are related to C-O vibration and the new synthesized compounds as shown in figure 2 clarifies the successful formation of Schiff base in stretching bands of C=N at 1615-1650 cm^{-1} in addition to disappearance of any aldehydic group.

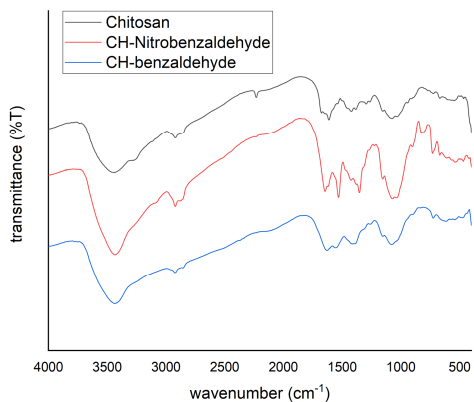


Figure 2: FTIR spectrum of chitosan and chitosan derivatives (CH-nitrobenzaldehyde and CH-Benzaldehyde)

3.1.1. FTIR Spectrum of m-nitrobenzaldehyde Chitosan

The schiff base stretching band vibration appears at 1644.98 cm^{-1} , nitro group stretching band appears at 1531.2 cm^{-1} and the aromatic C-H bending vibration bands appears at [680-730] cm^{-1} .

Table 2

Corrosion parameters of steel electrode in 0.24 M HCl solution containing different concentrations of inhibitors

Medium	Conc. (ppm)	β_a	$-\beta_c$	-E _{corr}	I _{corr}	IE%
Free		103	123.4	519.9	0.7663	-
Chitosan	200	60.2	82	522	0.4815	37.2
	400	54.3	65.2	530	0.2912	62
	600	67.4	127	492	0.2492	67.5
	800	47.2	81.97	516	0.2326	69.6
	1000	56.6	61.9	529	0.1255	83.6
m-Nitro Benzaldehyde	200	77.7	100.6	503	0.3168	43.2
	400	75.5	161.8	498.6	0.2724	56.5
	600	79.2	118.5	503.9	0.1792	61.3
	800	75.8	134	480	0.1769	75.2
	1000	68.6	150.4	467.7	0.0393	94.8
Benzaldehyde	200	74.4	87.7	528	0.2368	41.2
	400	87.5	113	527.6	0.2220	53.7
	600	61.5	116	503.8	0.1199	60.1
	800	79.8	97.6	504	0.0798	80.6
	1000	89.5	122	516	0.0268	96.5

3.1.2. FTIR Spectrum of benzaldehyde modified Chitosan

The schiff base stretching band vibration appears at 1628.59 cm^{-1} and the aromatic C-H bending vibration bands appears at [680-724] cm^{-1} .

3.2. Potentiodynamic polarization

Figure 3 shows the potentiodynamic polarization curves of mild steel in 0.24 M HCl in the absence and presence of various concentration of polymers. Corrosion potential (E_{corr}), anodic Tafel slopes (β_a), cathodic Tafel slopes (β_c), corrosion current density (I_{corr}), and inhibition efficiency are the potentiodynamic polarization characteristics (IE%)

The following equation was used to compute the inhibitory efficiency:

$$IE \% = (1 - (I_{inh}/I_{free})) * 100$$

When I_{inh} and I_{free} are the corrosion current of steel electrode in the presence and in the absence of inhibitors, respectively. The %IE increases with the increase of Concentration as shown in table 2.

Table 2 clearly shows that the addition of the chitosan compounds, we find that the change in the values β_a & β_c is low when compared to the blank solution. Also, E_{corr} values remain constant and shift in E_{corr} (≤ 11 mV). This confirms that the examined chitosan compounds are classified as an anti-corrosion of the mixed type.

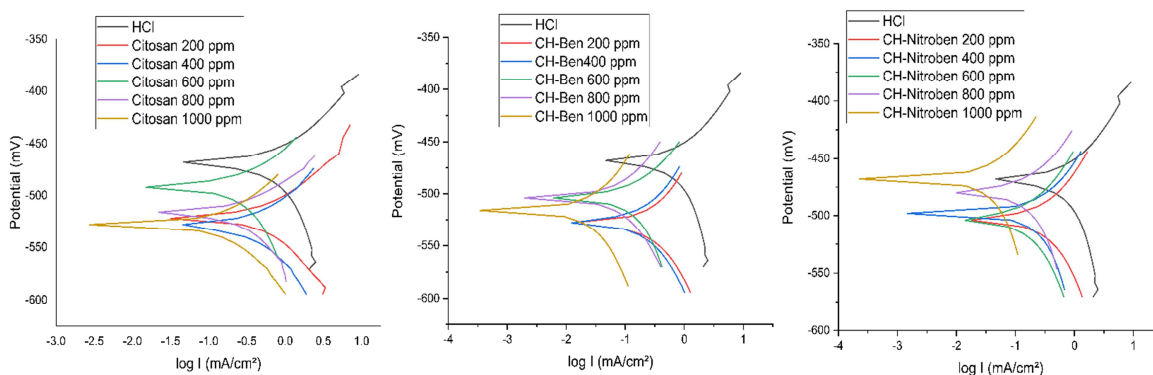


Figure 3: Anodic and cathodic polarization curves of steel electrode in 0.24 M HCl solution containing different concentration of Chitosan & CH-derivatives at 25°C.

3.2. Adsorption isotherm

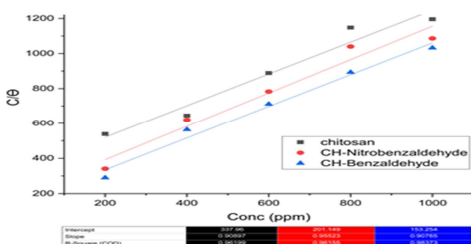


Figure 4: Langmuir adsorption isotherm of the adsorption of chitosan derivatives of the mild steel in 0.24M HCl at 25°C

The degree of surface coverage (θ) of steel surface by the adsorbed of compounds is calculated using the following equation.

$$\theta = 1 - \left(\frac{I_{inh}}{I_{free}} \right)$$

The corrosion current densities in the absence and presence of the additive's components, respectively, are I_{free} and I_{inh} . With increasing additive concentrations, the degree of surface coverage was found to increase. A number of mathematical relationships for the adsorption isotherms including Langmuir, Freundlich, Frumkin, Temkin have been suggested to fit the experimental data of the present work. The best results were obtained fitted Langmuir isotherm. Plotting C / θ versus inhibitor concentration (C) yields straight lines with unit slopes. This suggests that the inhibitors are adsorbing according to the Langmuir adsorption isotherm.

3.4. Effect of temperature

The temperature influence on corrosion parameters such as I_{corr} , E_{corr} , and %IE was investigated in a 0.24 M HCl solution containing 1000 ppm of inhibitors over temperature ranges of 25-65 °C. The results revealed that temperature change had essentially little influence on the form of the polarization curves. According to the data in Table 3, E_{corr} switched to fewer negative values as the temperature climbed, although I_{corr} values increased. This demonstrates that increased temperature has an accelerated influence on the corrosion response. Temperature increases, on the other hand, reduces inhibition efficiency. This is due to the accelerated desorption process caused by rising temperature.

Table 3

The effect of temperature on the corrosion parameters of steel electrode in 0.24 M HCl and (0.24M HCl + 1000ppm) of inhibitor

Compound	T(K)	-E _{corr}	I _{corr}	IE%
0.24 M HCl	298	519.9	0.7663	
	308	509.9	0.7835	
	318	506.5	0.8309	
	328	498.2	0.9335	
	338	494.8	0.9956	
Chitosan	298	528.6	0.1255	83.6
	308	527.4	0.2662	66
	318	512.5	0.3881	53.3
	328	518	0.4316	53.8
	338	523.6	0.5218	47.6
m-Nitro Benzaldehyde	298	470.7	0.0393	94.9
	308	470.5	0.1928	75.4
	318	427.9	0.2749	66.9
	328	460.2	0.4041	56.7
	338	447.6	0.4838	51.4
Benzaldehyde	298	524.1	0.0268	96.5
	308	506.9	0.1881	76
	318	516.7	0.223	73.2
	328	477.3	0.3654	60.9
	338	460.4	0.4815	51.6

The corrosion reaction is regarded as a rate process which is given by Arrhenius equation.

$$\log(I_{corr}) = \log(A) - Ea/2.303RT$$

Where I_{corr} represents the rate of corrosion reaction. A is Arrhenius factor and E_a is the apparent activation energy of the corrosion reaction. Plotting the $\log(I_{corr})$ versus $(1/T)$ gave straight lines in Fig (5).

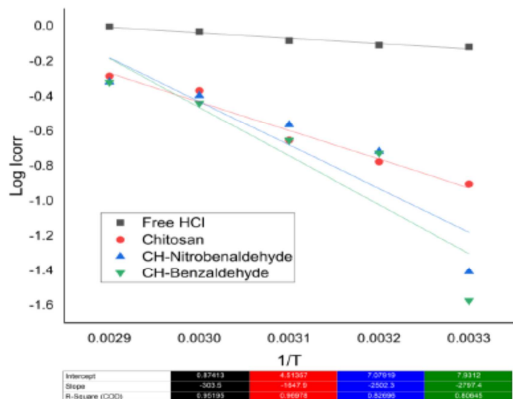


Figure 5: Arrhenius plots of steel corrosion rate in 0.24 M HCl in absence and presence of 1000 ppm of chitosan derivatives

The other activation parameters were calculated using the transition state equation:

$$\log\left(\frac{I_{corr}}{T}\right) = \left(\log(R/hn)\right) + \left(\frac{\Delta S^*}{2.303R}\right) - \left(\frac{\Delta H^*}{2.303RT}\right)$$

Where, R is the universal gas constant (8.314 J/mol.k), n is the Avogadro's number (6.02×10^{23}), h is the plank's constant ($6.62 \times 10^{-34} \text{ m}^2\text{kg/s}$) where ΔS^* and ΔH^* are the entropy and the enthalpy change, respectively. Plotting $\log(I_{corr}/T)$ versus $(1/T)$ gives straight lines Fig (6).

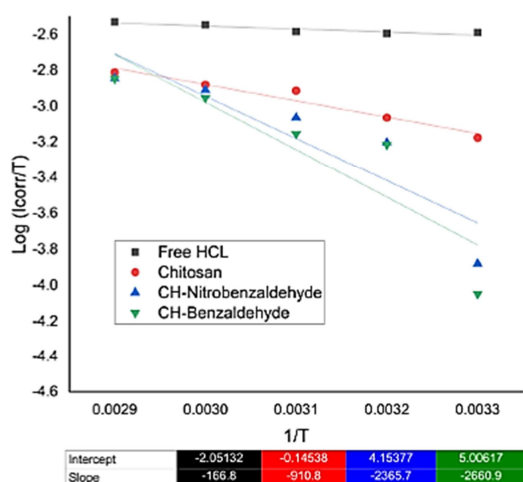


Figure 6: The relation between $\log(I_{corr}/T)$ and $1/T$ for steel electrode in 0.24 M HCl in absence and presence of 1000 ppm of compounds

Plotting $\log(I_{corr}/T)$ versus $(1/T)$ straight lines are obtained with a slope of $(-\Delta H^*)/(2.303R)$ and an intercept of $(\log(R/hn)) + ((\Delta S^*)/(2.303R))$ from which the values of ΔH^* and ΔS^* were calculated and are listed in Table (3). The change in the activation free energy (ΔG^*) of the corrosion process can be calculated at 298 K by applying the famous equation:

$$\Delta G^* = \Delta H^* - T\Delta S^*$$

The obtained ΔG^* values were also listed in Table (4).

Table 4

Activation parameters of the dissolution reaction of steel electrode in 0.24 M HCl solution in absence and presence of 1000 ppm of compounds

Compound	E_a K.J/mol. k	ΔH^* K.J/mol. k	$-\Delta S^*$ K.J/mol. k	ΔG^* K.J/mol. K
Free HCl	5.8	3.2	0.23686	73.78428
Chitosan	31.55	17.4	0.2	77
m-Nitro Benzaldehyde	28.76	24.6	0.18	78.24
Benzaldehyde	26.75	21.8	0.189	78.122

It is evident that the activation energy increases in the presence of the inhibitor, as a result of the inhibitor's adsorption on the metal's surface. The rise in E_a values is owing to the formation of adherent film on the mild steel surface. These outcomes demonstrate the physical adsorption of the chitosan compounds on the mild steel surface.

The positive sign of ΔH^* expresses the process's endothermic system, and the elevated values of E_a^* comparable to the values of ΔH^* indicate the corrosion process's gaseous nature, which can be easily explained by the evolution of hydrogen gas, which is accompanied by the volume decrease of the reaction[22].

The negative values of entropy ΔS^* refer to the increase of order and that attributed to the formation of metal-Chitosan complex which in turn decreases the freedom of the system.

3.5. Surface Examination

SEM shows the formation of corrosive layer in the case of mild steel immersed in 0.24M HCl for 3 days and the formation of protective layer by adding 1000 ppm of our new synthesised chitosan derivatives and immersed in 0.24M HCl for 3 days, and it is clear that the metallic surface appears less corroded[23].

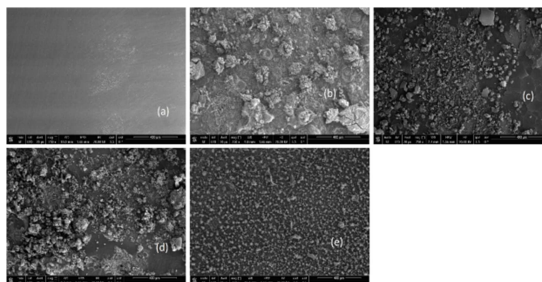


Figure 7 (a): SEM of mild steel surface (b) SEM of mild steel immersed in 0.24M HCl for 3 days. (c) SEM of mild steel immersed in 0.24M HCl for 3 days with 1000 ppm of chitosan. (d) SEM of mild steel immersed in 0.24M HCl for 3 days with 1000 ppm of CH-benzaldehyde. (e) SEM of mild steel immersed in 0.24M HCl for 3 days with 1000 ppm of CH-nitrobenzaldehyde

EDX curves show the decrease in weight% of oxygen and increase of weight% of Fe which reflects the efficiency of the added inhibitors comparable to the curve of mild steel in HCl.

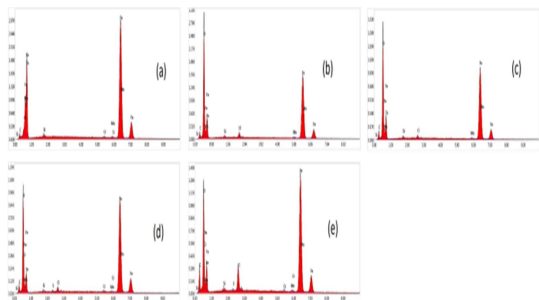


Figure 8 (a): EDX spectra of free mild steel. (b) EDX spectra of mild steel immersed in 0.24M HCl for 3 days. (c) EDX spectra of mild steel immersed in 0.24M HCl with 1000 ppm chitosan for 3 days. (d) EDX spectra of mild steel immersed in 0.24M HCl with 1000 ppm CH-benzaldehyde for 3 days. (e) EDX spectra of mild steel immersed in 0.24M HCl with 1000 ppm CH-nitrobenzaldehyde for 3 days

Conclusion

Using electrochemical measurements and scanning electron microscopy, the influence of Schiff base production of chitosan with benzaldehyde and m-nitrobenzaldehyde on the corrosion behavior of mild steel was investigated in this work. The freshly synthesized CH-derivatives have a greater corrosion prevention effect for mild steel in 0.24M HCl than Chitosan alone, according to this research.

In 0.24M HCl at 298 K, potentiodynamic polarization curves and Energy Dispersive X-Ray Analysis (EDX) data demonstrated that chitosan coated substrates had superior corrosion inhibition behavior than bare mild steel. In 0.24M HCl solution, the inhibitory efficiency (IE) was observed to reach 96.5%.

References

1. Bouklah, M., et al., *Thiophene derivatives as effective inhibitors for the corrosion of steel in 0.5 M H₂SO₄*. Journal of Applied Electrochemistry, 2005. **35**(11): p. 1095-1101.
2. Azhar, M., et al., *Corrosion inhibition of mild steel by the new class of inhibitors [2,5-bis(n-pyridyl)-1,3,4-thiadiazoles] in acidic media*. Corrosion Science, 2001. **43**: p. 2229-2238.
3. M. Abdallah, A. Fawzy, and A. Al Bahir, **Expired amoxicillin and cefuroxime drugs as efficient anticorrosives for Sabcic iron in 1.0 M hydrochloric acid solution**. Chem.Eng.Comm.,209(2)(2022)158-170..
5. M. Abdallah, Kamal A. Soliman, Rami Alfattani, Arey J Al-Gorair, A. Fawzy, Mahmoud A. A.

Ibrahim, Insight of corrosion mitigation performance of SABIC iron in 0.5 M HCl Solution by tryptophan and histidine: Experimental and computational approaches, Int. J. of Hydrogen Energy, 47(2) (2022)12782-12797.

6. Reda Abdel Hameed, Ayham Essa, Dina Mohamed, Metwally Abdallah, Meshari Aliohani, Saedah Al-Mhyawi, Mahmoud Soliman, Enas Ismail Arafa .Evaluation of expired augmentine drug as corrosion inhibitor for carbon steel alloy in 1.0NHCl acidic environment using analytical techniques. *Egypt J. of Chemistry* ,65 (4)(2022) pp. 735 – 745
7. Heise, S., et al., *Electrophoretic deposition of chitosan/bioactive glass/silica coatings on stainless steel and WE43 Mg alloy substrates*. Surface and Coatings Technology, 2018. **344**: p. 553-563.
8. Clavijo, S., et al., *Electrophoretic deposition of chitosan/Bioglass® and chitosan/Bioglass®/TiO₂ composite coatings for bioimplants*. Ceramics International, 2016. **42**(12): p. 14206-14213.
9. Al-Rashidy, Z.M., et al., *Orthopaedic bioactive glass/chitosan composites coated 316L stainless steel by green electrophoretic co-deposition*. Surface and Coatings Technology, 2018. **334**: p. 479-490.
10. Boccaccini, A.R., *Electrophoretic deposition: fundamentals and applications in materials science*. Journal of Materials Science, 2006. **41**(24): p. 8029-8030.
11. Carneiro, J., J. Tedim, and M.G.S. Ferreira, *Chitosan as a smart coating for corrosion protection of aluminum alloy 2024: A review*. Progress in Organic Coatings, 2015. **89**: p. 348-356.
12. M. Abdallah K.A. Soliman, Arey S Al-Gorair, A. Al Bahir , Jabir H. Al-Fahemi, M.S.Motawea, Salih S. Al-Juaid, *Enhancing the inhibition and adsorption performance of SABIC iron corrosion in sulfuric acid by expired vitamins. Experimental and computational approach*, *RSC Advances*,11 (2021)17092–17107.
13. Mobin, M., R. Aslam, and J. Aslam, *Non toxic biodegradable cationic gemini surfactants as novel corrosion inhibitor for mild steel in hydrochloric acid medium and synergistic effect of sodium salicylate: Experimental and theoretical approach*. Materials Chemistry and Physics, 2017. **191**.
14. John, S., et al., *Enhancement of corrosion protection of mild steel by chitosan/ZnO nanoparticle composite membranes*. Progress in Organic Coatings, 2015. **84**: p. 28-34.
15. Fekry, A., *Acetyl thiourea chitosan as an eco-friendly inhibitor for mild steel in sulphuric acid medium*. Electrochimica Acta, 2010. **55**: p. 1933-1939.
16. Cui, G., et al., *Chitosan oligosaccharide derivatives as green corrosion inhibitors for P110 steel in a carbon-dioxide-saturated chloride solution*. Carbohydrate Polymers, 2019. **203**: p. 386-395.
17. El-Haddad, M.N., *Chitosan as a green inhibitor for copper corrosion in acidic medium*.

- International Journal of Biological Macromolecules, 2013. **55**: p. 142-149.
18. Wan, K., et al., *Enhanced corrosion inhibition properties of carboxymethyl hydroxypropyl chitosan for mild steel in 1.0 M HCl solution*. RSC Advances, 2016. **6**(81): p. 77515-77524.
 19. Solomon, M.M., et al., *Gum Arabic-silver nanoparticles composite as a green anticorrosive formulation for steel corrosion in strong acid media*. Carbohydrate Polymers, 2018. **181**: p. 43-55.
 20. John, S., et al., *Corrosion inhibition of mild steel using chitosan / TiO₂ nanocomposite coatings*. Progress in Organic Coatings, 2019. **129**: p. 254-259.
 21. Feng, P., et al., *Synergistic protective effect of carboxymethyl chitosan and cathodic protection of X70 pipeline steel in seawater*. RSC Advances, 2017. **7**(6): p. 3419-3427.
 22. Appa Rao, B.V. and S.S. Rao, *Synergistic Inhibition of Corrosion of Carbon Steel by the Ternary Formulations containing Phosphonate, Zn (II) and Ascorbic Acid*. Research Journal of Recent Sciences, 2012. **1**(ISC-2011): p. 93-98.
 23. Tang, J., et al., *Corrosion behaviour of carbon steel in different concentrations of HCl solutions containing H₂S at 90°C*. Corrosion Science, 2011. **53**(5): p. 1715-1723.